Rendiconti
Accademia Nazionale delle Scienze detta dei XL
Memorie di Scienze Fisiche e Naturali
136° (2018), Vol. XLII, Parte II, Tomo II, pp. 47-59

ANTONIO LAGANÀ[1,2] – FERNANDO PIRANI[1] – NOELIA FAGINAS LAGO[1]
GIUSEPPE VITILLARO[2] – ERNESTO GARCIA[3]

Process driven potentials for Open Molecular Science Cloud computational services: the nitrogen case study

Abstract – The paper aims to illustrate the ongoing work to develop Open Molecular Science Cloud services for Astrochemistry enabling distributed computational molecular simulations based on the formulation of the potential energy of their reactive and non reactive state selected elementary components. To this end the paper leverages experimental and theoretical information supporting the building of reliable descriptors of the potential energy, the singling out of the channels driving the dynamical behaviour of the molecular system and the characterizing of the energy dependence of the efficiency of the occurring elementary collisions. In particular, the paper focuses on the advantage of using potential energy surfaces combining longer range (Improved Lennard-Jones) and shorter range (Bond Order) functional forms targeting the full range description of the evolution of the chemical process from asymptotes inward to strong interaction regions and from internal regions backward to the (same or different) asymptote. As a case study we examine here some nitrogen based systems and discuss the connection between the features of the used potential energy surface and some improvements proposed to their currently used formulation.

[1] Dipartimento di Chimica, Biologia e Biotecnologie, Università di Perugia, 06100 Perugia, Italy. E-mail: lagana05@gmail.com
[1] Dipartimento di Chimica, Biologia e Biotecnologie, Università di Perugia, 06100 Perugia, Italy. E-mail: Fernando.Pirani@unipg.it
[1] Dipartimento di Chimica, Biologia e Biotecnologie, Università di Perugia, 06100 Perugia, Italy. E-mail: noelia.faginaslago@unipg.it
[2] CNR ISTM - UOS Perugia, 06100 Perugia, Italy. E-mail: giuseppe@vitillaro.org
[3] Departamento de Quimica Fisica, Universidad del Pais Vasco (UPV/EHU), 01006 Vitoria, Spain. E-mail: e.garcia@ehu.es

1. *Introduction*

The assemblage of appropriate Potential Energy Surfaces (PES)s is of key importance for the accurate evaluation of the dynamics and kinetics properties of molecular systems of interest for astrochemistry [1]. The computational procedure adopted for this purpose is usually articulated into a) the production and/or collection of high resolution experimental and high level ab initio theoretical information on the electronic structure of the involved molecular system, b) the fitting of available data using a suitable formulation of the PES, c) the checking, correcting and coding the PES into a high performing routine, d) the calculation of an extended set of detailed dynamical quantities and their averaging to evaluate the desired observable.

We have already incorporated the steps of the above mentioned procedure into the so called Grid Empowered Molecular Simulator (GEMS) [2-4] implemented as an activity of the Virtual Organization (VO) COMPCHEM [5] first and of the Chemistry Molecular and Materials Science and Technologies (CMMST) Virtual Research Community (VRC) [6] later. According to the dictate of the Open Science consultation document [see ref. 7] we are driving the CMMST VRC Molecular science modelers to adopt an Investigating → Discovering → Analysing → Writing → Publishing → Outreaching → Assessing approach via the development of a dedicated Open Science cloud solution. This is aimed at creating common interfaces and standard maintenance, interoperability and sustainability procedures for data, protocols and methodologies [see http://ec.europa.eu/research/openscience/] for the purpose of offering to everybody the possibility of computing both accurate structural data for chemical compounds and ab initio efficiency parameters for chemical processes.

More specifically, in the recent past, GEMS has been used for the systematic study of the homonuclear chemical processes of Nitrogen. Within this effort, full-dimensional PESs of $N + N_2$ [starting with a LEPS published in ref. 8] were produced. In particular, their Largest-Angle Generalized ROtating Bond Order (LAGROBO) formulation [9] based on Bond Order (BO) coordinates [10] has been used to fit a double barrier Minimum Energy Path (MEP) shown by a set of available high-level ab initio data [11, 12]. Further ab initio calculations were performed later and two new full-dimensional PESs were produced [13, 14] both confirming a double barrier shape of the $N + N_2$ MEP. The investigation was also extended to $N_2 + N_2$ by focusing on the inelastic channel. Accordingly, the PES was formulated as a sum of N_2 intramolecular and intermolecular interactions formulated in terms of distances, spherical harmonics and bond-bond pairwise additive interactions [see for example refs 15-18]. Both the inelastic channel and the LAGROBO approaches were extended also to four nitrogen atom systems. Studies of the interaction components of $N_2 + N_2$ have been reported in [refs. 19-21]. In order to include in the study the switch to atom exchange and fragmentation processes further ab initio

studies were performed for a large set of molecular geometries [22-24] and fitted using also a statistically localized, permutationally invariant, local moving least squares interpolating function [25, 26]. These studies provided also a fitted PES (MN) for the N + N_2 system bearing sufficient flexibility to improve the quality of dynamical studies and to allow a valid description of higher energy processes (including dissociation) [27] even if it cannot be accredited of the necessary accuracy for the calculation of low temperature thermal rate coefficients and low energy detailed state specific collision induced cross sections due to the lack of an attractive long range tail [28]. On the contrary, both the already mentioned Double Many Body Expansion (DMBE) PES [14] and an hybrid LAGROBO and Improved Lennard-Jones [29] (ILJ) PES exhibit an attractive long range tail.

Accordingly, the paper is articulated as follows: in section 2 the evolution towards the provision of cloud services is briefly illustrated, in sections 3 the method adopted for the full range formulation of the potential energy of the two body N-N system is discussed, in section 4 the process-driven method adopted for formulating the full range three body N + N_2 LAG4ILJ PES is discussed, in section 5 the force field approach used for the N_2 dimer is discussed, in section 6 some quantum dynamical effects depending on the inclusion of an accurate long range tail in the N + N_2 potential energy surface are reported, in section 7 some Molecular Dynamics features of the N_2 dimer leveraging the ILJ formulation of the N-N long range interaction and coulombic terms are reported.

2. *The Molecular Science computational platform evolution towards the provision of cloud services*

The work aimed to develop a dedicated Open Science cloud infrastructure for the Molecular Science community started thanks to the COST [www.cost.eu/] Action D23 METACHEM [www.cost.eu/COST_Actions/cmst/D23] launched by the University of Perugia in the year 2000. METACHEM was able to connect the activities of different Molecular Science research laboratories on a shared computing platform made of a geographically distributed cluster of heterogeneous computers connected as a single virtual parallel machine [30]. Grid solutions and paradigms for molecular science research developed by D23 were further enhanced by the next COST Action D37 (Grid Computing in Chemistry: GRIDCHEM) started in the year 2006. GRIDCHEM leveraged the creation and the use of distributed computing infrastructures (the «Grid») to drive collaborative computer modelling and simulation in chemistry towards «new frontiers in complexity and a new regime of time-to-solution» [31].

As a matter of fact, about ten years ago the European projects EGEE [Enabling Grids for E-sciencE, https://cordis.europa.eu/project/rcn/87264_en.html] first and EGI [European Grid Infrastructure, https://en.wikipedia.org/wiki/European-Grid-Infrastructure] later provided European researchers with a world class level platform

for computational collaborations. In particular, during the EGEE-III project, a pilot distributed computational application was assembled to demonstrate the possibility of implementing grid techniques for performing accurate calculations of cross sections and rate coefficients of reactive and non reactive molecular processes for a very large number of molecular geometries [32] and collisional events [33]. This fostered the establishing of the already mentioned COMPCHEM VO[5] and the generalization of the distributed procedures computing the cross sections and the rate coefficients of reactive and non reactive molecular processes into GEMS[2]. This also provided the proper ground for establishing (in the year 2013) a network of (mainly European even if not only) Chemistry Departments sharing their on-line educational services (e-test, learning objects, on-line courses, etc.) leveraging an open collaborative user/producer (Prosumer) [34] model and prompted the assembling at the Dipartimento di Chimica, Biologia e Biotecnologie (DCBB) of the University of Perugia of an embryonic cloud platform of the Beowulf type, named HERLA [https://en.wikipedia.org/wiki/Beowulf_cluster]. The platform consisted in a couple of HPC clusters, (CG/training) and (FE/research), running Scientific Linux 6.x, with two distinct access nodes. The clusters were connected using NIS in a single-image system, and were used the first for students' training (CG) and the second (FE) for scientists' research. Two years later the CMS[2] Consortium of the University of Perugia, of CNR ISTM - UOS Perugia and of the two companies Master-UP srl and Molecular Horizon srl took over the management of HERLA.

More recently cloud images of HERLA (VHERLA) were created and in collaboration with the Department of Physics and Geology (DFG) and INFN Perugia were deployed on a CEPH storage (locate at DCBB) to support the activities of the School Open Science Cloud (SOSC17) held in Perugia on June 2017 and running under the INFN OpenStack platform. The next step of the process consisted in allocating a Virtual Data Center on the GARR Cloud to the end of generating a virtual cluster for Molecular Sciences, with the support of A. Barchiesi (GARR CSD) and G. Attardi (GARR Cloud).

3. *The formulation of the two body N + N potential energy*

A popular formulation of the potential energy of a chemical system for dynamical studies is the one combining locally appropriate (dominant) analytical representations of the interaction by means of appropriate (possibly physically meaningful) switching function (say $g(r)$) turning on and off the various components depending of the value of the internuclear distance r. The obvious starting point of our investigation was the formulation of the potential $V^{(2)}(r)$ of two body (nuclei) systems (here we obviously refer to the Nitrogen-Nitrogen (N-N) one due to the already specified focus of the paper). In the two body problem one can easily compose the $V^{(2)}(r)$ potential (let's call it $V^{(2\text{-}tot)}(r)$ for that purpose) as

$$V^{(2\text{-}tot)}(r) = V^{(2\text{-}spectr)}(r)g(r) + V^{(2\text{-}scatt)}(r)(1 - g(r)). \quad (1)$$

The first term of the sum $V^{(2\text{-}spectr)}(r)$ is usually formulated as a Morse potential

$$V^{(2\text{-}spectr)}(r) = V^{(morse)}(r) = D_e(n^2 - 2n) = D_e(1 - n)^2 - De \quad (2)$$

in which D_e is the dissociation energy of the diatom and $n = \exp(-\gamma\ (r\text{-}r_e))$ is the already mentioned BO variable with γ being a constant proportional to the square root of the force constant of the oscillator. A more flexible formulation of $V^{(2\text{-}spectr)}(r)$ is obtained by the generalization of the Morse functional form to higher powers of n as follows

$$V^{(2\text{-}spectr)}(r) = V^{(BO)}(r) = De \sum_{j=0}^{J} c_j n^j. \quad (3)$$

The value of the c coefficients of eq. 3 are either derived by fitting accurate high level ab initio calculations (see Table 1 for the N-N diatom) or by working out them from spectroscopic force constants [see ref. 35 for the adopted procedure].

Table 1. Coefficients of the N_2 BO potentials formulated using D_e=228.23 kcal/mol and r_e=1.098 Å. The RMSD of BO4 and BO6 from the ab initio data of ref. 36 are 1.035 kcal/mol and 0.650 kcal/mol respectively.

PES	c_1	c_2	c_3	c_4	c_5	c_6
BO_4	2.4200	-1.9573	0.6547	-0.1174		
BO_6	2.9833	-3.7743	2.9145	-1.4858	0.4077	-0.0457

As to the second term of $V^{(2\text{-}tot)}(r)$ (i.e. the $V^{(2\text{-}scatt)}(r)$) it is the already mentioned ILJ potential [29] defined below

$$V^{(2\text{-}scatt)}(r) = V^{(ILJ)}(r) = \varepsilon_o \left[\frac{m}{s(x) - m} \frac{1}{x^{s(x)}} - \frac{s(x)}{s(x) - m} \frac{1}{x^m} \right]. \quad (4)$$

In eq. 4 where $x = r/r_e$, $s(x) = \beta + 4x^2$ (with β ranging from 6 to 10 depending on the hardness of the interacting electronic distributions which is proportional to the cubic root of the polarizability α of the interacting partners). For N-N both ε_o and r_e can also be derived from the polarizability of the interacting partners. The values used for our calculations are: m = 6, ε_o = 6.43 meV, r_e = 3.583 Å and β=6.6055. The BO and the ILJ potentials allow a smooth matching between the atom-atom (scattering) long range and the diatom (spectroscopy) short range components of the formulation of the total two body interaction $V^{(2\text{-}tot)}(r)$ without resorting to a complex formulation of the $g(r)$ switching function. This is useful when dealing with insufficiently dense sets of ab initio electronic structure values.

The formulation of a proper switching function $g(r)$, however, is an important factor for an appropriate connection of the two components of $V^{(2\text{-}tot)}(r)$. The first consideration to make to this end is that $V^{(2\text{-}spectr)}(r)$ and $V^{(2\text{-}scatt)}(r)$ refer, indeed, to different arrangements of the electrons around the nuclei with a strongly bound (the first) and a weakly (or non) bound (the second) nature respectively. Accordingly, n (the BO variable) and x (the reduced ILJ radius) provide clear boundaries ($n = 1$ and $x = 1$) for the interval within which locate the switching function $g(r)$. Within that interval we can either adopt a symmetrically switching function or pilot the switching through the minimum difference between $V^{(2\text{-}spectr)}(r)$ and $V^{(2\text{-}scatt)}(r)$. We are also considering the possibility of adopting a formulation coupling two adiabatic-like components of $V^{(2\text{-}tot)}(r)$ and exploiting high level (experimental and theoretical) information on ionization and polarization energies.

4. *Process Driven Fitting Methods for three body N + N_2 interactions*

The functional representation of the three N atom (N_{L-1}, N_L and N_{L+1}) potential for the $N_{L-1} + N_{L(L+1)} \rightarrow N_{(L-1)L} + N_{(L+1)}$ reactive channel at fixed value of the angle Φ_L (the angle formed by the internuclear distances $r_{L/1,L}$ and $r_{L,L+1}$) can be formulatd in terms of the polar BO coordinates ρ_L and η_L defined (see Fig. 1) as:

$$\rho_L = \left[n^2_{(L-1)L} + n^2_{L(L+1)} \right]^{1/2} \tag{5}$$

and

$$\eta_L = \tan^{-1} \left[\frac{n_{(L-1)L}}{n_{L(L+1)}} \right] \tag{6}$$

using the so called ROtating BO (ROBO) [37] model. In this case one can set the origin of the axes at $n = 0$ (that is at $r = \infty$) for the two involved BO variables without artificial loss of flux. The angle η_L (see Fig. 1) can be taken as a continuity variable in the transformation of the reactant diatom $L(L + 1)$ of channel L into the related product one $(L - 1)L$. At the same time the variable ρ_L (see again Fig. 1) spans the different fixed arrangement angle Φ_L elongations of the system. The corresponding fixed arrangement angle Φ_L ROBO potential channel(s), can be formulated as a polynomial in ρ_L as follows:

$$V_L^{BO}(\Phi_L; \eta_L, \rho_L) = D(\Phi_L; \eta_L) P(\Phi_L; \eta_L; \rho_L) \tag{7}$$

in which $D(\Phi_L; \eta_L)$ represents the fixed collision angle Φ_L depth of the process channel evolving from reactants (at $\eta_L = 0$) to products (at $\eta_L = \pi/2$) while the polynomial $P(\Phi_L, \eta_L; \rho_L)$ represents the shape of the L channel cut while the system elongates (or contracts) out of its (fixed η_L) minimum energy geometry. In the particular case of N + N_2 discussed in ref. 19 the following simple formulation

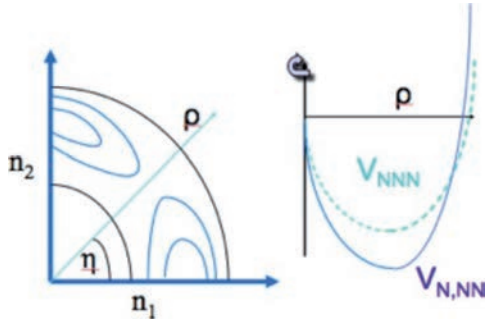

Fig. 1. LHS PLOT: Qualitative isoenergetic contours of the single barrier N+N_2 LAGROBO PES; RHS PLOT: Cuts of the reaction channel at the asymptotes (blue line) and at the saddle (green line) of the N+N_2 LAGROBO PES. For simplicity we drop here the L index for ρ and η and we name n_1 and n_2 the BO variables $n_{L-1,L}$ and $n_{L,L+1}$.

$$D(\Phi_L;\, \eta_L) = -D_e + S_{L1}(\Phi_L)\, \sin(2\eta_L) \tag{8}$$

was adopted to the end of fitting the single barrier of the LEPS thanks both to the collinearity ($\Phi_L^{TS} = 180°$) of the transition state (TS) and to the homonuclear symmetry of the system. In this case, in eq. 8, S_{L1} is equal to the value of the potential energy of the collinear saddle E^{TS}. Corrective S_{Lj} terms depending on the deviation of the actual value of Φ_L from the saddle Φ_L^{TS} one were then added when moving away from the collinear arrangement. In addition, further corrective S_{Lj} terms having the form:

$$S_{Lj} = \sum_{k=1}^{kmax} E^{TS}\, (\Phi_{Lk}^{TS} - \Phi_L)^{2(k\text{-}1)} \tag{9}$$

for the given value of Φ_L were added to the end of changing the topology of the minimum energy path (for example from single to double well). Furthermore, in order to consider all the possible process channels of the system, we combined different fixed Φ_L ROBO formulations into a single LAGROBO (Largest Angle Generalized ROBO) full 3D one and incorporated the long range tail of the potential using an ILJ potential suitably modified to deal with a pseudo-atom diatomic body of the relevant channel. This means that at a value of η_L corresponding to a sufficiently large value of R_{N-N2} (the atom-diatom internuclear distance hereafter called just R) an ILJ potential in R was formulated [29] as:

$$V(R,\, \gamma) = \varepsilon(\gamma) \left\{ \frac{m}{s(R,\, \gamma) - m} \left[\frac{R_m(\gamma)}{R} \right]^{s(R,\gamma)} - \frac{s(R,\, \gamma)}{s(R,\, \gamma) - m} \left[\frac{R_m(\gamma)}{R} \right]^{m} \right\} \tag{10}$$

where $\varepsilon(\gamma)$ and $R_m(\gamma)$ represent, respectively, the depth of the van der Waals potential well and its location in R. In eq 10, the first term describes the R-dependence of

the repulsion, while the second one represents the R-dependence of the long-range attraction with $s(R, \gamma) = \sigma + 4[R/R_m(\gamma)]^2$ and σ being a factor related to the hardness of the two interacting partners. For all values of the orientation angle γ the potential parameters are defined as $R_m(\gamma) = R_{m\perp} \cos^2 \gamma + R_{m\parallel} \sin^2 \gamma$ and $\varepsilon(\gamma) = \varepsilon_\perp \cos^2 \gamma + \varepsilon_\parallel \sin^2 \gamma$, with the $\perp$ and $\parallel$ symbols representing the perpendicular and the collinear arrangements of the system.

By including the ILJ term into the fourth PES of the LAGROBO series the so called LAG4ILJ PES having the advantage of fitting in the most appropriate way both the short and the long-range sets of *ab initio* data was generated. In particular, in the short-range region the calculations were confined, as already mentioned, around the process channel (avoiding so far to compute the (large) fraction of *ab initio* values falling in the forbidden regions) and in the long range region (out of the van der Waals well) concentrate the efforts in best fitting the relevant model parameters.

5. *The Force field of the N_2 dimer*

To realistically describe the total interaction potential energy of the N_2 dimer we had to add the electrostatic (V_{elec}) component to the non-electrostatic (V_{nelec}) one. As discussed earlier the non electrostatic part is properly represented by the already mentioned ILJ potential [29] whereas the electrostatic part is calculated as a simple Coulombic potential

$$V_{tot}(R) = V_{nelec}(R) + V_{elec}(R) = V_{ILJ}(R) + V_{Coul}(R). \quad (11)$$

We can either place the molecular interaction centre on the centre of mass of N_2 to reduce the molecule to a pseudo-atom bearing the total molecular polarizability (CM-CM model) or take into separate account the effects of atomic polarizabilities by means of atom-atom 4 ILJ terms as follows:

$$V_{nelec}(R_{AB}) = \sum_{i,j=1}^{2} V_{ILJ}(R_{ij}) = V_{ILJ}(R_{11}) + V_{ILJ}(R_{21}) + V_{ILJ}(R_{12}) + V_{ILJ}(R_{22}) \quad (12)$$

where i and j indicate the nitrogen atoms of the N_2 molecules A and B within the dimer. This type of potential will be referred to as atom-atom potential.

For the simulation of small gaseous molecules, often partial charges are introduced in the system to calculate the electrostatic interaction. Although such partial charges do not have an actual physical meaning, they are usually chosen so as to best fit a molecular property (often the lowest non-zero multipole is chosen for that purpose). The parameters of the ILJ potential were optimized using different charge schemes. For the N_2 gas, usually either a three site or a four site charge system is adopted [38]. The three-charge system has negative charges on the N atoms and a

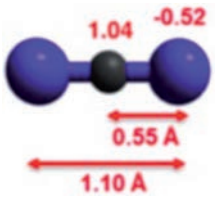

Fig. 2. The charges' scheme adopted to reproduce the electrostatic term of the interaction.

balancing charge on the centre of mass twice the amount needed to get an overall neutral molecule. The negative charges are placed at a distance of 1.10Å from each other, while the positive charge is displaced at a distance of 0.55Å (see Fig. 2). An electrostatic energy contribution is then calculated as the Coulombic sum

$$V_{Coul}(R) = \sum_{i,j} \frac{qiqj}{R_{ij}} \tag{13}$$

where i and j are the relevant point charges located in the N_2 dimer and follow the notation of eq. 12.

6. *The N + N_2 quantum dynamics*

Quantum state to state inelastic probabilities were calculated using the program ABC [39] based on the time-independent hyperspherical coordinate integration of the atom diatom Schrödinger equation for all the reactant states lower than the total energy E_{tot} and a fixed value of the total angular momentum quantum number J. To this end, ABC expands the system wavefunction into a basis set of fixed hyperradius ρ (not to be confused with the above defined BO coordinate ρ) hyperangular functions. The integration is performed by segmenting the ρ interval into several sectors and propagating through them the scattering **S** matrix (from 0 to an asymptotic ρ_{max} value (16 Å)) where the probability **P** matrix is evaluated. Extended convergency checks were performed at total angular momentum J=0 for the overall elastic and inelastic collisions. The analysis of the quantum values of the J=0 probability associated with inelastic transitions from a given initial rovibrational v, j state to a given final v' vibrational (summed over all rotational) states (v,j|v',all) computed on the DMBE, MN and LAG4ILJ PESs shown in Fig. 3 allows us to accurately quantify the efficiency of the vib-rotational-to-vibrotational energy transfer without resorting to approximations. An important conclusion of such analysis in the energy range of up to 1 eV is the clear predominance of vibrationally elastic events over vibrational excitation and deexcitation. The importance of including the long range tail (as is for the LAG4ILJ PESs) is shown, however, by the enhancement of the efficiency of the vibrational excitation computed on LAG4ILJ of at least one order of magnitude over the DMBE PES and two orders of magnitude over the MN PES and in the corresponding lowering of the energy threshold.

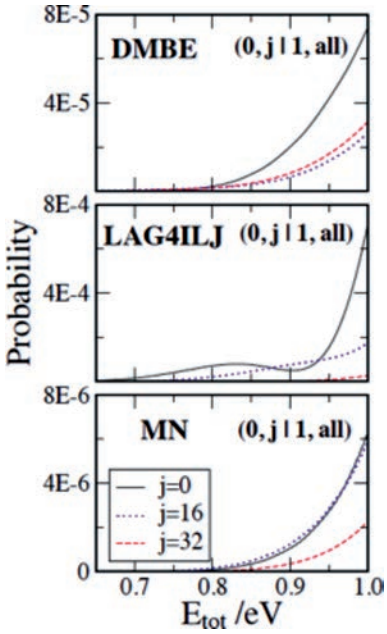

Fig. 3. (v,j|v',all) inelastic transition probabilities computed on the DMBE (upper panel), LAG4ILJ (central panel) and MN (lower panel) PESs plotted as a function of total energy at $J = 0$ and $j = 0, 16, 32$.

A more systematic analysis of the structure of the computed probabilities is given by the comparison of the probability for transitions from a given initial rotational state j to a final

Table 2. Interaction parameters for the N_2 dimer using an atom-atom model.

Charge scheme	ε (kcal/mol)	r_0 (Å	β	q^-(e)
no charges				
no charges	0.074	3.893	8.033 /	
Three Charge model				
This work	0.081	3.770	9.000	-0.52

j´ one (only jumps of two units are allowed by the symmetry of the system) as a function of j. These probabilities clearly indicate that there is a tendency of the system to rotationally excite N_2 and trigger a self-sustained rotational excitation of N_2.

7. *Molecular Dynamics of the N_2 dimer*

Molecular Dynamics (MD) simulations of the N_2 dimer have been performed in the canonical (NVT) ensemble using the DL_POLY program [40]. The size of the simulation box was of 36.11 x 62.52 x 140.00 Å3. A Nose-Hoover thermostat with a relaxation constant of 0.5 ps has been employed to keep the temperature T of the system fixed at 300 K. The cutoff distance for the nonelectrostatic and electrostatic components has been set to 15 Å, and the Ewald method has been applied for the calculation of electrostatic contributions. During the simulations the membrane structure was kept frozen and the gas molecules treated as rigid. Each simulation has been performed for 5 ns after a properly long equilibration period with a fixed time step of 1 fs by collecting data every 2 ps. After each production run, the trajectories were recorded and the results analyzed. The simulation temperatures fluctuated between 20 and 3 percent (relative standard deviations vary from 7% to 1%) in going from lower to higher pressure. We consider here first the case of a single interaction centre located on the centre of mass of the N_2 molecule. The interaction parameters are given in Table 2 with relevant partial charges. It is clear from the Table that an explicit inclusion of the electrostatic term by means of the Coulombic sum only affects the ILJ parameters when large charges are used.

Table 3. Interaction energies (D_e) and equilibrium distance (r_{i0}) of the N_2 dimer calculated by the molecular dynamics simulation compare with the literature.

Charge scheme	D_e(kcal/mol)	r_0 (Å)
no charges		
no charges	0.293	3.78
Three Charge model		
Optimized [43]	0.222	3.94
CCSD T [44]	0.205	3.57
This work	0.2635	3.69

In this case, the introduction of the electrostatic term changes the parameters less than in the CM-CM model. For the three-charge model, ε and r_0 increase slightly with the increase of charges (while β decreases). The optimized charges are again slightly higher than the ones reported in the literature. The computed ε and r_0 values for the ILJ potential are similar to those of the relevant Lennard-Jones one (notice the different symbols). Ravikovich *et al.* have reported values of 0.202 kcal/mol for ε and 4.058Å for r_0 of the LJ CM-CM model with no charges [41]. Those ε and r_0 are higher than ours. The agreement is, though, reasonable when taking into account that they were obtained using a completely different method. We can compare the ε and r_0 parameters of the atom-atom model directly to the TraPPE and MOM LJ

ones for the three-charge model [42]. The ε and r_0 for both the MOM and the TraPPE potential (0.072 kcal/mol and 3.730Å respectively) compare reasonably well with our values. Furthermore, we can compare to ILJ parameters using the three-charge model [see ref. 43]. They obtained optimized values of 0.079 kcal/mol, 3.897Å and 7.720 for ε, r_0 and β respectively when using a charge of -0.5664 on the N atom.

In order to examine the performances of the different approaches, the interaction energies of some highly symmetrical configurations of the N_2-dimer were calculated with the different interaction potentials fitted. The values are presented in Table 3. Three representative configurations (T-shape, parallel and linear) were taken into account and were compared with the interaction energies computed at the CCSD(T)/CBS [44] level, which is a well-recognized standard for evaluating the accuracy of other computational methods. From Table 3 it can be seen that the interaction energies of N_2-dimers calculated with the different fittings are in general in good agreement with the CCSD(T) results for the considered noncovalent interaction.

REFERENCES

[1] Talbi D. (2011). Theoretical approaches for studying Astrochemistry, EPJ Web of Conferences, 18: 02002.
[2] Laganà A., Costantini A., Gervasi O., Faginas Lago N., Manuali C., Rampino S. (2010). J. Grid Comput., 8: 571-586.
[3] Manuali C., Laganà A., Rampino S. (2010). Computer Physics Communications, 181: 1179-1185.
[4] Rampino S., Faginas Lago N., Laganà A., Huarte-Larrañaga F. (2012). Journal of Computational Chemistry 33: 708-714.
[5] Costantini A., Gervasi O., Faginas Lago N., Manuali C., Rampino S. (2010). Journal of Grid Computing, 8(4): 571-586.
[6] Laganà A. (2012). http://www.hpc.unipg.it/ojs/index.php/virtlcomm/article/view/40.
[7] http://ec.europa.eu/research/consultations/science-2.0/science_2_0_final_report.pdf.
[8] A. Laganà A., Garcia E., Ciccarelli L. (1987). J. Phys. Chem., 91: 312–314.
[9] Garcia E., Laganà A. (1995). J. Chem. Phys. 103: 5410-5416.
[10] Johnston H.S., Parr C. (1963). J. Am. Chem. Soc., 85: 2544.
[11] Garcia E., Laganà A. (1997). J. Phys. Chem., 101: 4734-4740.
[12] Garcia E., Saracibar A., Gómez-Carrasco S., Laganà A. (2008). Phys. Chem. Chem. Phys., 10: 2552-2558.
[13] Wang D., Stallcop J.R., Huo W.M., Dateo C.E., Schwenke D.W., Partridge H. (2003). J. Chem. Phys., 118: 2186-2189.
[14] Galvão B.R.L., Varandas A.J.C. (2009). J. Phys. Chem., 113: 14424-14430.
[15] van der Avoird A., Wormer P.E.S., Jansen A.P.J. (1986). J. Chem. Phys. 84: 1629-1635.
[16] Gomez L., Bussery-Honvault B., Cauchy T., Bartolomei M., Cappelletti D., Pirani F. (2007). Chem. Phys. Lett., 445: 99-107.
[17] Hellmann R. (2013). Mol. Phys., 111: 387-401.
[18] Cappelletti D., Pirani F., Bussery-Honvault B., Gomez L., Bartolomei M. (2008). Phys. Chem. Chem. Phys., 10: 4281-4293.

[19] Verdicchio M. (2009). Atmospheric reentry calculations and extension of the formats of quantum chemistry data to quantum dynamics, Master Thesis University of Perugia.
[20] Kurnosov A., Cacciatore M., Laganà A., Pirani F., Bartolomei M., Garcia E. (2014). J. Comput. Chem., 35: 722.
[21] Garcia E., Martínez T., Laganà A. (2015). Chem. Phys. Lett., 620: 103.
[22] Pacifici L., Verdicchio M., Faginas Lago N., Lombardi A., Costantini A. (2013). J. Comput. Chem., 34: 2668-2676.
[23] Paukku Y., Yang K.R., Varga Z., Truhlar D.G. (2013). J. Chem. Phys., 139: 044309.
[24] Paukku Y., Yang K.R., Varga Z., Truhlar D.G. (2014). J. Chem. Phys., 140: 019903.
[25] Bender J.D., Doraiswamy S., Truhlar D.G., Candler G.V. (2014). J. Chem. Phys., 140: 054302.
[26] Bender J.D., Valentini P., Nompelis I., Paukku Y., Varga Z., Truhlar D.G., Schwartzentruber T., Candler G.V. (2015). J. Chem. Phys., 143: 054304.
[27] Esposito F., Garcia E., Laganà A. (2017). Plasma Sources Science and Technology 26(4): 045005.
[28] Garcia E., Aoiz F.J., Rampino S., Laganà A. (2018) Quantum state-to-state inelastic probabilities in N + N2 collisions: the role of the respulsive wall and the long-range interaction, Frontiers in Chemistry, section Physical Chemistry and Chemical Physics (abstract accepted for publication).
[29] Pirani F., Brizi S., Roncaratti L., Casavecchia P., Cappelletti D., Vecchiocattivi F. (2008). Phys. Chem. Chem. Phys., 10: 5489.
[30] Foster I., Kesselman C. Eds., The Grid: Blueprint for a New Computing Infrastructure, Morgan Kaufmann Publ., San Francisco (1999).
[31] https://www.cost.eu/actions/D37/#tabs|Name:overview
[32] Storchi L., Tarantelli F., Laganà A. (2006). Lecture Notes in Computer Science 3980: 675-683.
[33] Gervasi O., Laganà A. (2004). Future Generation Computer Systems, 20(5): 703-716.
[34] Laganà A., Gervasi O., Tasso S., Perri D., Franciosa F. (2018). Lecture Notes in Computer Science 10964: 533-548.
[35] Garcia E., Laganà A. (1985). Mol. Phys. 56: 621-627.
[36] Varandas A.J.C. (1980). J. Chem: Soc. Faraday II, 76: 129.
[37] Laganà A. (1991). J. Chem. Phys. 95: 2216.
[38] Makrodimitris K., Papadopoulos G.K., Schober H., Theodorou D.N. (2001). J. Phys. Chem. B, 105: 777–788.
[39] Skouteris D., Castillo J.F., Manolopulos D.E. (2000). Comp. Phys. Comm. 133: 128-135.
[40] Smith W., Yong C.W., Rodger P.M. (2002). Molecular Simulation, 28(5): 385-471.
[41] Ravikovitch P.I., Vishnyakov A., Neimark A.V. (2001). Phys. Rev. E, 64(1).
[42] Murthy C.S., Singer K., Klein M.L., Mcdonald I. R. (1980). Mol. Phys. 41(6): 1387-1399.
[43] Vekeman J., Faginas-Lago N., Cuesta I.G., Sánchez-Marín J., De Merás A.S. (2018). Lecture Notes in Computer Science, 10964.
[44] Tian L., Feiwu C. (2013). J. Mol. Model. (19)12, 5387-5395.